International Journal of Civil Engineering

Structural Engineering

Optimal design of barrel vaults using charged search system

A. Kaveh[1,*], **M. Farahani**[2], **N. Shojaei**[3]

Received: October 2011, Accepted: January 2012

Abstract

Barrel vaults are attractive space structures that cover large area without intermediate supports. In this paper, the charged search system (CSS) optimization algorithm is employed for optimal design of barrel vaults. This method utilizes the governing laws of Coulomb and Gauss from electrostatics and the Newtonian law of mechanics. The results demonstrate the efficiency of the discrete CSS algorithm compared to other meta-heuristic algorithms.

Keywords: Heuristic optimization algorithm; Charged system search; Optimal design of barrel vaults.

1. Introduction

Braced barrel vault systems provide long span economical roof structures to give large unobstructed floor areas [1]. Many bracing configurations are available and each system has a different stiffness and response to the imposed loading. These structures are sensitive to support conditions and also to non-symmetrically imposed loading which tends to govern the design of barrel vaults. The structural performance of a long single-layer barrel vault can be greatly enhanced by the inclusion of transverse stiffening ribs. Single-layer barrel vaults, primarily spanning longitudinally, are more efficient at high height-to-transverse-span ratios and their behavior is analogous to an assembly of trusses. Barrel vaults with shallow rises must be checked to ensure that local and overall instability does not occur. Of the single-layer barrel vaults analyzed, the three-way grid type has proven to give the most uniform stress distribution throughout the structure, and due to the low number of joints required in comparison with other configurations, results in the most economical structural system. The use of double-layer barrel vaults enhances the stiffness of the structure and provides structural system of great potential capable of having spans exceeding 100 m.

The term optimization is related to a field of research in which one minimizes or maximizes a function by systematically selecting the values of variables from an acceptable set. In one hand, a great deal of research has been performed in this area of knowledge, aspiring to plan noticeable and efficient optimization algorithms. On the other hand, the application of the existing algorithms to real projects has also been the focus of many studies.

In the past, most commonly applied optimization techniques have been gradient-based algorithms that utilize gradient information to find for the solution space. Most of the gradient-based methods compared to stochastic approaches converge faster and gain solutions with higher accuracy. However, the acquisition of gradient information to obtain minima can be either costly or even impossible. Furthermore, this kind of algorithms is only guaranteed to converge to local minima. Also, there should be a good starting point for a successful execution of these methods. In many optimization problems, prohibited zones, side limits and non-smooth or non-convex functions must be implemented and considered. As a result, these non-convex optimization problems can not be solved by these methods. Other types of optimization methods, known as meta-heuristic algorithms (Fugal et al. [2]; Holland [3]; Goldberg [4]; Glover [5]; Dario et al. [6]; Eberhart and Kennedy [7]; Kirkpatrick et al. [8]; Geem [9]; Erol and Eksin [10]; Kaveh and Talatahari [11-13], Kaveh and Sbzi [14]; Kaveh and Nasr [15]; Kaveh et al. [16]), are not restricted in the aforementioned manner. These methods are suitable for global search due to their capability of detecting and finding promising regions in the search space at an affordable time. Meta-heuristic algorithms tend to perform well for most of the optimization problems. The reason is that these methods avoid simplifying or making assumptions about the original problem. Evidence of this is their successful utilization to a vast variety of fields, such as engineering, art,

* *Corresponding Author: alikaveh@iust.ac.ir*
1Professor, Centre of Excellence for Fundamental Studies in Structural Engineering, Iran University of Science and Technology, Narmak, Tehran-16, Iran
2M.Sc. Iran Sadra Institute of Higher Education, Tehran, Iran
3M.Sc. School of Civil Engineering, Iran University of Science and Technology, Tehran-16, Iran

biology, economics, marketing, genetics, operations research, robotics, social sciences, physics, politics and chemistry.

The remainder of this paper is organized as follows. Section 2 presents a background of the laws utilized in CSS. The main rules of the method are explained in section 3. In section 4, optimal design of barrel vaults is presented. In Section 5 elastic critical load analysis of spatial structures is presented. Section 6 studies various design examples to verify the efficiency of the CSS. A discussion and conclusion is presented in section 7.

2. Background

A recently developed meta-heuristic algorithm is the charged system search (CSS) introduced by Kaveh and Talatahari [11]. This method utilizes the governing laws of Coulomb and Gauss from electrostatics and the Newtonian law of mechanics. CSS uses a number of charged particles (CPs) which affect each other based on their fitness values and separation distances. By these laws, a model is created to regulate the structural optimization method. CSS involves a number of agents (CPs), and each CP is considered as a charged sphere which implements an electric force on other CPs according to the Coulomb and Gauss laws. The resultant forces and the motion laws determine the new location of the CPs. Utilizing these laws, provides a good balance between the exploration and the exploitation of the algorithm. Different types of skeletal structures are considered to exhibit the efficiency of the CSS algorithm, Kaveh and Talatahari [12].

Electrical laws

In physics, the space surrounding an electric charge has a property known as the electric field. This field imposes a force on other electrically charged objects. The electric field surrounding a charged point is given by Coulomb's law. Coulomb has shown that the electric force between two small charged spheres is proportional to the inverse square of their separation distance r_{ij}. Thus Coulomb's law provides the magnitude of the electric force (Coulomb force) between every two point charges. This force on a charge, q_j at position r_j , experiencing a field due to the presence of another charge, q_i at position r_i , can be expressed as

$$\mathbf{F}_{ij} = k_e \frac{q_i q_j}{r_{ij}^2} \frac{\mathbf{r}_i - \mathbf{r}_j}{\| \mathbf{r}_i - \mathbf{r}_j \|} \tag{1}$$

where k_e is a constant known as the Coulomb constant; r_{ij} is the separation of the two charges, Halliday et al. [17]. Consider an insulating solid sphere of radius a that has a uniform volume charge density and freights a total charge of magnitude q_i. The magnitude of the electric force at a point outside the sphere is determined by Eq. (1), while this force can be obtained using Gauss's law at a point inside the sphere as

$$\mathbf{F}_{ij} = k_e \frac{q_i q_j}{a^3} r_{ij} \frac{\mathbf{r}_i - \mathbf{r}_j}{\| \mathbf{r}_i - \mathbf{r}_j \|} \tag{2}$$

$$\mathbf{F}_j = \sum_{i=1, i \neq j}^{N} \mathbf{F}_{ij} \tag{3}$$

where N is the total number of charged particles and F_{ij} is equal to

$$\mathbf{F}_{ij} = \begin{cases} \dfrac{k_e q_i}{a^3} r_{ij} \dfrac{\mathbf{r}_i - \mathbf{r}_j}{\| \mathbf{r}_i - \mathbf{r}_j \|} & \text{if } r_{ij} < a \\ \dfrac{k_e q_i}{r_{ij}^2} \dfrac{\mathbf{r}_i - \mathbf{r}_j}{\| \mathbf{r}_i - \mathbf{r}_j \|} & \text{if } r_{ij} \geq a \end{cases} \tag{4}$$

Therefore, the resulted electric force can be obtained as

$$\mathbf{F}_j = k_e q_j \sum_i \left(\frac{q_i}{a^3} r_{ij} \cdot i_1 + \frac{q_i}{r_{ij}^2} \cdot i_2 \right) \frac{\mathbf{r}_i - \mathbf{r}_j}{\| \mathbf{r}_i - \mathbf{r}_j \|} \quad \begin{matrix} i_1 = 1, i_2 = 0 \Leftrightarrow r_{ij} < a \\ i_1 = 0, i_2 = 1 \Leftrightarrow r_{ij} \geq a \end{matrix} \tag{5}$$

Newtonian mechanics studies the motion of objects. In general, a particle is a point- like mass containing infinitesimal size. The motion of a particle is completely known if the particle's position in space is known at all times. The displacement of a particle is defined as its change in position. As it is transferred from an initial position and rolled to a final position renew, its displacement is given by

$$\Delta \mathbf{r} = \mathbf{r}_{new} - \mathbf{r}_{old} \tag{6}$$

The slope of tangent line of the particle position represents the velocity of this particle as

$$\mathbf{v} = \frac{\mathbf{r}_{new} - \mathbf{r}_{old}}{t_{new} - t_{old}} = \frac{\mathbf{r}_{new} - \mathbf{r}_{old}}{\Delta t} \tag{7}$$

The acceleration of the particle is defined as the change in the velocity divided by the time interval Δt during which that change has occurred:

$$\mathbf{a} = \frac{\mathbf{v}_{new} - \mathbf{v}_{old}}{\Delta t} \tag{8}$$

Also according to Newton's second law, we have

$$\mathbf{F} = m \cdot \mathbf{a} \qquad \mathbf{r}_{new} = \frac{1}{2} \frac{\mathbf{F}}{m} \cdot \Delta t^2 + \mathbf{v}_{old} \cdot \Delta t + \mathbf{r}_{old} \tag{9}$$

3. The rules of the charged system search

The rules of the CSS are presented briefly in the following:

Level 1: Initialization

• Step 1: Initialization. Initialize the CSS algorithm parameters; Initialize an array of Charged Particles (CP) with random positions and their associated velocities (Rules 1 and 2).

• Step 2: CP ranking. Evaluate the values of the fitness function for the CPs, compare with each other and sort in an increasing order.

• Step 3: Charged Memory (CM) creation. Store CMS=*N/4* number of the first CPs and their related values of the objective functions in the CM, where N is the number of CPs.

Level 2: Search

• Step 1: Attracting force determination. Determine the probability of moving each CP toward others (Rule 3), and calculate the attracting force vector for each CP (Rule 4).

• Step 2: Solution construction. Move each CP to the new position and find the velocities (Rule 5).

• Step 3: CP position correction. If each CP exits from the

allowable search space, correct its position using Rule 7.

• Step 4: CP ranking. Evaluate and compare the values of the objective function for the new CPs, and sort them in and increasing order.

• Step 5: CM updating. If some new CP vectors are better than the worst ones in the CM, include the better vectors in the CM and exclude the worst ones from the CM (Rule 6).

Level 3: Terminating criterion controlling

• Repeat search level steps until a terminating criterion is satisfied (Rule 8 the flowchart of the CSS algorithm is demonstrated in Fig. 1.

4. Optimal design of barrel vaults

Minimizing the structural weight W requires the selection of the optimum values of number cross-section di while satisfying the design constraints. The discrete optimal design problem of truss structure may be expressed as

Find :

$$X = [x_1, x_2, \ldots x_{ng}] \tag{10}$$

To minimize :

$$W(X) = \sum_{i=1}^{nm} \gamma_i . x_i . l_i \tag{11}$$

Subject to:

$$\begin{aligned} & x_i \in D_i, D_i = \left\{ d_{i,1}, d_{i,2}, \ldots\ldots d_{i,r(i)} \right\} \\ & \delta_{\min} \le \delta_i \le \delta_{\max} \quad i = 1, 2..., m \\ & \sigma_{\min} \le \sigma_i \le \sigma_{\max} \quad i = 1, 2..., nm \end{aligned} \tag{12}$$

where X is a vector containing the design variables; D_i is an allowable set of discrete values for the design variable x_i; ng is the number of design variables or the number of member groups; $r(i)$ is the number of available discrete values for the i th design variable; $W(X)$ is the cost function which is taken as the weight of the structure; nm is the number of members forming the structure; m is the number of nodes; γ_i is the material density of member i; L_i is the length of the member i; σ_i and δ_i are the stress and nodal displacement, respectively;

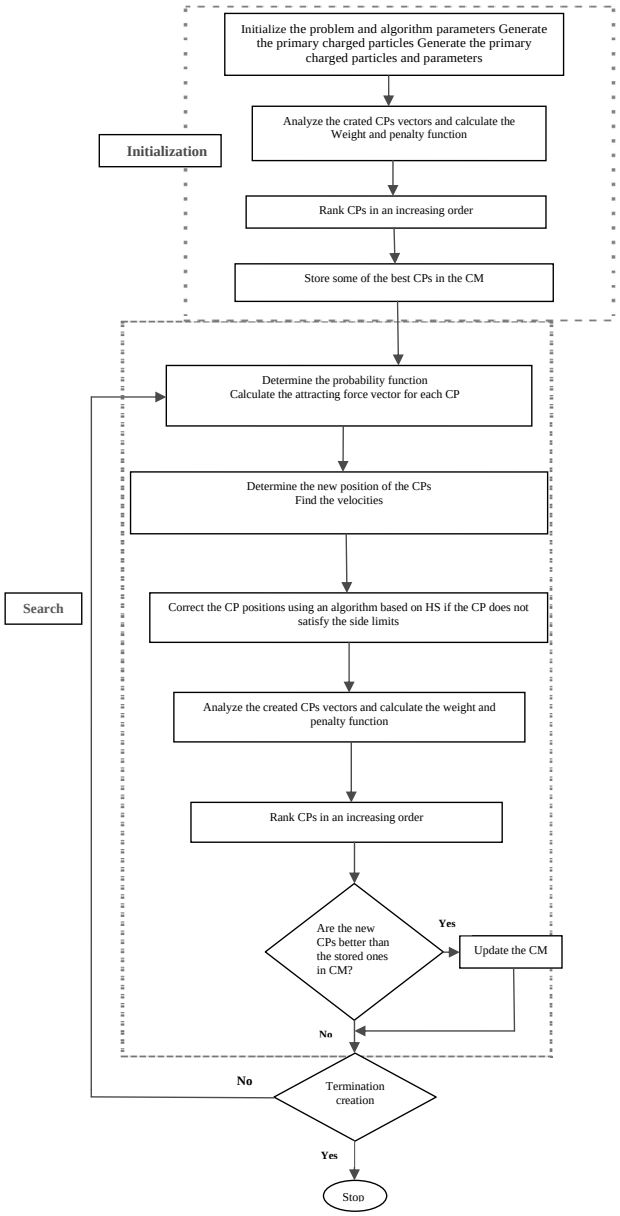

Fig. 1. The flowchart for the CSS algorithm [11-12]

5. Elastic critical load analysis of spatial structures

The rigidity of joints has a great influence on the stress distribution in single-layer braced barrel vaults. The experiments show that large span slender single-layer braced barrel vaults are prone to instability, especially under the action of heavy unsymmetrical loads, and that the rigidity of joints exerts an important influence on the overall stability of the structure. The barrel vault structures are rigid structures for which the overall loss of stability might take place when these structures are subjected to equipment loading concentrated at the apex. Therefore, the stability check is vital during the analysis to make sure that the structure does not lose its load carrying capacity due to instability and otherwise, considering the nonlinear behavior in the design of the barrel vaults is necessary because of the change in geometry under external loads. Rigid joints modify the deflections and the stress distribution greatly in single layer braced barrel vaults. The results obtained assuming pin-connected joints differ appreciably from those calculated for rigid joints. If the members are relatively long, then the stability failure will be by simple member buckling while if the members are relatively short so that members meeting at a joint are nearly coplanar, then a snap through buckling mode involving more than one member will dominate. The buckling mode may involve just one node or a group of nodes, or possibly the entire structure.

Details of the elastic instability analysis of a barrel vault with rigid connections are listed in the following:

Step 1: Set the load factor to a pre-selected initial value and assume the axial forces in members are equal to zero.

Step 2: Compute the stability functions using the current values of axial forces in the members.

Step 3: Set up the nonlinear stiffness matrix for each member.

Step 4: Transform the member stiffness matrices from local

coordinates into the global coordinate system and assemble the overall stiffness matrix.

Step 5: Check the stability of the barrel vault. Calculate the determinant of the overall stiffness matrix. If it becomes negative, then the barrel vault becomes instable and the design process is terminated; otherwise, go to the next step.

Step 6: Analyze the barrel vault under the factored external loads and obtain the joint displacements.

Step 7: Find the member forces.

Step 8: Replace the previous axial forces in members with the new ones.

Step 9: Repeat the steps from 2 until differences between two successive sets of axial forces are smaller than a specific tolerance.

Step 10: Increase the load factor by pre-selected value. If the load factor has reached to the specified ultimate value, terminate the elastic critical load analysis; otherwise, go to Step 2.

Many different schemes of diagonal bracings can be chosen from a wide variety of configurations. These configurations may be broadly categorized as triangular and rectangular. Plans of some of the configuration that are often chosen are used in this paper. Moreover, single-layer barrel vault with a three-way triangular configuration deflect much less under non-symmetrical loads than do other types.

6. Design examples

In this section, the optimal design of two barrel vaults is performed by CSS algorithm. The final results are compared to the solutions of other methods to demonstrate the efficiency of the present approach. Sections are selected from the allowable steel pipe sections taken from LRFD-AISC shown in Table 1.

Loading condition

The two loading conditions are considered:

Case 1. The vertical downward load; [(D+S)]

Case 2. The vertical downward load and wind load directions; [D+S+W]

Weight of sheeting = 10 kg/m^2

Estimated weight of space frame, purlin, nodes and stubs =25 kg/m^2

D = Total dead load=35kg/m^2

S = Snow load=80kg/m^2

W =Wind load= negative internal pressure = –84.5 kg/m^2

W =Wind load= positive internal pressure =+33.8 kg/m^2

W =Wind load= negative internal pressure = –169 kg/m^2

6.1. Example 1: A 237-bar barrel vault

There are several possible types of bracings used in the construction of single-layer braced barrel vaults in steel, aluminum or timber. The geometry and nodal numbering of a typical barrel vault is shown in Fig. 2. For the 237-bar barrel vault the material density is taken as 0.288 lb/in^3 (7971.8 kg/m^3) and the modulus of elasticity is 30,450 ksi (210,000 MPa). The members are subjected to the stress limits of +34.8, –22.5 ksi. Structural members of this barrel vault are categorized into 15 groups using symmetry: (1) A1 - A11, (2) A12 - A21, (3) A22 - A31, (4) A32 - A41, (5) A42 - A52, (6) A53 - A61, (7) A62 - A73, (8) A74 - A83, (9) A84 - A105, (10) A106 - A127, (11)

Table 1. The allowable steel pipe sections taken from LRFD-AISC

	Type	Nominal diameter (in.)	Weight	Area(cm^2)	Area (in.^{2})	I (in.^{4})	S (in.^{3})	J (in.^{4})	Z (in.^{3})
1	ST	1/2	0.85	1.61	0.250	0.017	0.041	0.082	0.059
2	EST	1/2	1.09	2.06	0.320	0.020	0.048	0.096	0.072
3	ST	3/4	1.13	2.14	0.333	0.037	0.071	0.142	0.100
4	EST	3/4	1.47	2.79	0.433	0.045	0.085	0.170	0.125
5	ST	1	1.68	3.18	0.494	0.087	0.133	0.266	0.187
6	EST	1	2.17	4.12	0.639	0.106	0.161	0.322	0.233
7	ST	1 1/4	2.27	4.31	0.669	0.195	0.235	0.470	0.324
8	ST	1 1/2	2.72	5.15	0.799	0.310	0.326	0.652	0.448
9	EST	1 1/4	3.00	5.68	0.881	0.242	0.291	0.582	0.414
10	EST	1 1/2	3.63	6.90	1.07	0.666	0.561	1.122	0.761
11	ST	2	3.65	6.90	1.07	0.391	0.412	0.824	0.581
12	EST	2	5.02	9.54	1.48	0.868	0.731	1.462	1.02
13	ST	2 1/2	5.79	10.96	1.70	1.53	1.06	2.12	1.45
14	ST	3	7.58	14.38	2.23	3.02	1.72	3.44	2.33
15	EST	2 1/2	7.66	14.51	2.25	1.92	1.34	2.68	1.87
16	DEST	2	9.03	17.16	2.66	1.31	1.10	2.2	1.67
17	ST	3 1/2	9.11	17.29	2.68	4.79	2.39	4.78	3.22
18	EST	3	10.25	19.48	3.02	3.89	2.23	4.46	3.08
19	ST	4	10.79	20.45	3.17	7.23	3.21	6.42	4.31
20	EST	3 1/2	12.50	23.74	3.68	6.28	3.14	6.28	4.32
21	DEST	2 1/2	13.69	25.99	4.03	2.87	2.00	4.00	3.04
22	ST	5	14.62	27.74	4.30	15.2	5.45	10.9	7.27
23	EST	4	14.98	28.45	4.41	9.61	4.27	8.54	5.85
24	DEST	3	18.58	35.29	5.47	5.99	3.42	6.84	5.12
25	ST	6	18.97	35.99	5.58	28.1	8.50	17.0	11.2
26	EST	5	20.78	39.41	6.11	20.7	7.43	14.86	10.1
27	DEST	4	27.54	52.25	8.10	15.3	6.79	13.58	9.97
28	ST	8	28.55	54.19	8.40	72.5	16.8	33.6	22.2
29	EST	6	28.57	54.19	8.40	40.5	12.2	24.4	16.6
30	DEST	5	38.59	72.90	11.3	33.6	12.1	24.2	17.5
31	ST	10	40.48	76.77	11.9	161	29.9	59.8	39.4
32	EST	8	43.39	82.58	12.8	106	24.5	49.0	33.0
33	ST	12	49.56	94.19	14.6	279	43.8	87.6	57.4
34	DEST	6	53.16	100.64	15.6	66.3	20.0	40.0	28.9
35	EST	10	54.74	103.87	16.1	212	39.4	78.8	52.6
36	EST	12	65.42	123.87	19.2	362	56.7	113.4	75.1

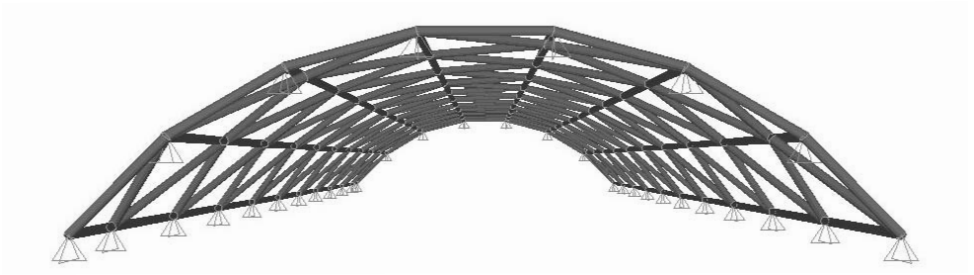

(a)

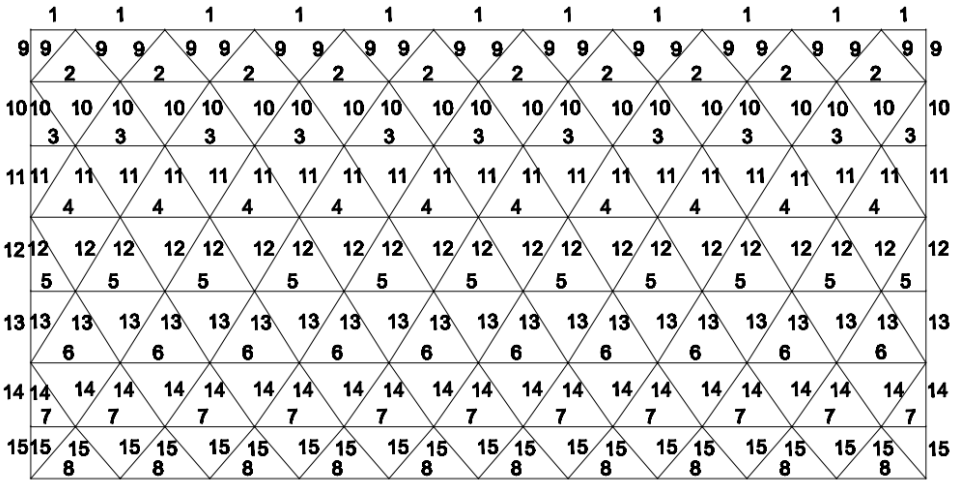

(b)

Fig. 2. (a) The front view of the 237-bar barrel vault, (b) Nodal numbering of 237-bar barrel vault

A128 - A149, (12) A150 -A171, (13) A172 - A193, (14) A194 - A215, (15) A216 - A237. The minimum permitted cross-sectional area of each member is ST1/2 0.25 in^2 (1.61 cm^2), and the maximum cross-sectional area of each member is EST5 6.11 in2 (39.41 cm^2), [18, 19]. Table 2 provides the values and directions of the two load cases applied to the 237-bar barrel vault. The convergence history of this barrel vault is shown in Fig. 3. The best weight of the CSS optimization is 30213.7356 lb (13707 kg), while it is 31066.8442 lb (14092 kg), 30876.7478 lb (14005.45 kg), for the GA and PSO, respectively.

6.1.1. Configuration of the 237-bar barrel vault:

Consider the barrel vault shown in Fig. 2.
R=Radius=152.4 in (387 cm)
H=Height=59 in (150 cm)
L=Length=480 in (1219 cm)
D=Span= 240.15 in) 610 cm)

The performance comparsion for the 237-bar barrel vault is provide in Table 3.

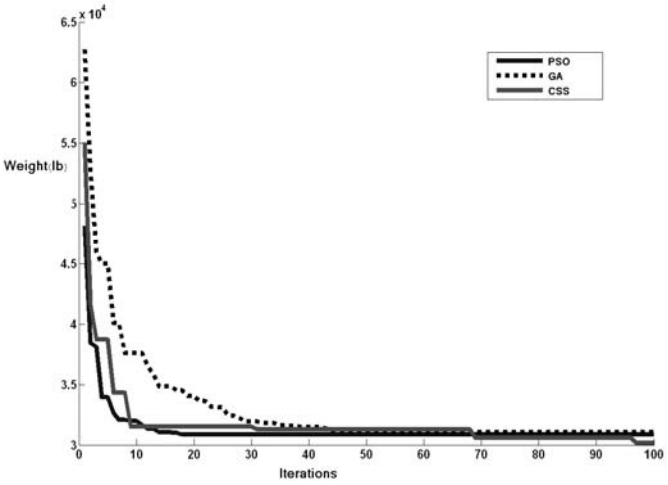

Fig. 3. The convergence history of the double layer 237-bar barrel vault

Table 2. Loading conditions for the 237-bar barrel vault

Node	Case 1			Case 2		
	Px kips(kN)	Py kips(kN)	Pz kips(kN)	Px kips(kN)	Py kips(kN)	Pz kips(kN)
63	0	0	−0.3206(1.42)	0	0.450(2)	−0.2082(0.92)
64	0	0	−0.3206(1.42)	0	0.450(2)	−0.2082(0.92)
65	0	0	−0.3206(1.42)	0	0.450(2)	−0.2082(0.92)
66	0	0	−0.3206(1.42)	0	0.450(2)	−0.2082(0.92)

6.2. Example 2: An 888-bar barrel vault

The geometry of the barrel vault is shown in Fig. 4. For an 888-bar barrel vault the material density is 0.288 lb/in^3 (7971.8 kg/m^3) and the modulus of elasticity is taken as 30,450 ksi (210,000 MPa). The members are subjected to the stress limits of +34.8, ˜ 22.5 ksi. Structural members of this barrel vault are categorized into 38 groups using symmetry. The minimum permitted cross-sectional area of each member is ST 1/2(0.25 in^2) (1.61 cm^2), and the maximum cross-sectional area of each member is ST10 (11.90 in^2) (76.7 cm^2). Table 4 provides the values and directions of the two load cases applied to this barrel vault. The best weight of the CSS optimization is 60852.6106 lb (27602 kg), while it is 61844.7728 lb (28052.31 kg), 61183.313 lb (27752.2 kg), for the GA and PSO, respectively.

6.2.1. Configuration of 888-bar barrel vault:

R=Radius=1295 in (3289 cm)
H=Height=255.9 in (650 cm)
L=Length=1588.5 in (4035 cm)
D=Span=1545.2 in (3925 cm)

The Performance comparsion for the 888 bar barrel vault is provide in Table 5. The convergence history of this barrel vault is shown in Fig. 5.

Table 3. Performance comparsion for the 237-bar barrel vault

Element group		Optimal cross-sectional areas (in2)		
		GA	PSO	CSS
1	A1~ A11	EST 1 1/4	ST 1 1/4	EST 1 1/4
2	A12~A21	ST 4	ST 4	DEST 3
3	A22~A31	ST 3	ST 1 1/4	ST 1
4	A32~A41	EST 4	EST 3 1/2	EST 5
5	A42~A52	ST 1 1/4	EST 1 1/2	ST 1 1/2
6	A53~A61	ST 4	EST 4	ST 3
7	A62~A73	DEST 2 1/2	ST 4	EST 4
8	A74~A83	EST 3	EST 2	ST 2 1/2
9	A84~A105	EST 3	ST 3 1/2	ST 3 1/2
10	A106~A127	ST 5	EST 4	DEST 3
11	A128~A149	DEST 2 1/2	EST 5	EST 4
12	A150~A171	EST 3	EST 3	ST 3 1/2
13	A172~A193	ST 3 1/2	EST 2 1/2	EST 2
14	A194~A215	ST 4	ST 3	EST 2 1/2
15	A216~A237	EST 2 1/2	ST4	ST 2 1/2
Best weight lb(kg)		**31066.8442(14092)**	**30876.7478(14005.4)**	**30213.7356(13707)**

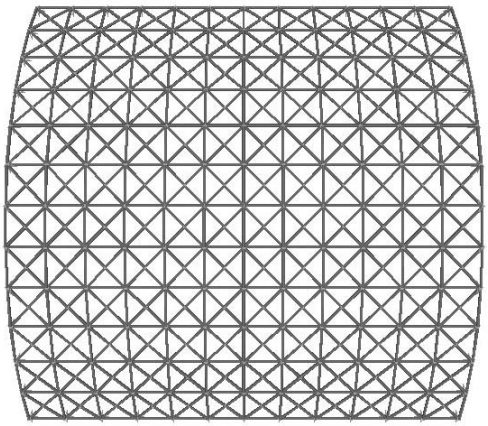

Fig. 4. Top view of 888-bar barrel vault

Table 5. Performance comparsion for the 888-bar barrel vault

Element group		Optimal cross-sectional areas (in^2)		
		GA	PSO	CSS
1	A1~ A12	DEST 2	EST 2 1/2	ST 1/2
2	A13~A24	ST 2 1/2	EST 5	EST 2 1/2
3	A25~A36	ST 1 1/4	EST 1 1/2	EST 1 1/4
4	A37~A48	EST 1 1/2	ST 1/2	EST 5
5	A49~A60	EST 1 1/4	EST 1 1/2	ST 1/2
6	A61~A672	ST 3 1/2	ST 1/2	ST 1/2
7	A73~A84	EST 3	DEST 2	ST 3 1/2
8	A85~A96	ST 3	ST 1/2	EST 4
9	A97~A108	EST 1 1/4	EST 3/4	ST 1/2
10	A109~A120	ST 3/4	ST 1/2	ST 3
11	A121~A132	EST 2	ST 1/2	ST 1/2
12	A133~A144	EST 1 1/4	ST 5	ST 6
13	A145~A156	EST 1 1/4	ST 1/2	ST 3
14	A157~A169	ST 1 1/4	ST 1 1/2	ST 3 1/2
15	A170~A182	EST 1 1/4	ST 4	ST 1/2
16	A183~A195	ST 5	ST 4	ST 1/2
17	A196~A208	ST 3	ST 3 1/2	ST 1/2
18	A209~A221	ST 10	ST 1/2	ST 4
19	A222~A234	DEST 2 1/2	EST 3	ST 2 1/2
20	A235~A247	ST 2 1/2	ST 1/2	ST 1/2
21	A248~A260	EST 1 1/2	EST 2 1/2	EST 4
22	A261~A273	ST 5	EST 2 1/2	ST 1/2
23	A274~A286	EST 1 1/4	ST 3/4	ST 1/2
24	A287~A299	ST 1	ST 1	DEST 2
25	A300~ A312	ST 4	EST 4	ST 1/2
26	A313~A336	ST 1/2	ST 1/2	ST 1/2
27	A337~A384	ST 1/2	ST 1/2	ST 1/2
28	A385~A432	ST 1/2	ST 1/2	ST 1/2
29	A433~A480	ST 1/2	ST 1/2	ST 1/2
30	A481~A528	ST 1/2	ST 1/2	ST 1/2
31	A529~A576	ST 1/2	ST 1/2	ST 1/2
32	A577~A624	ST 1/2	ST 1/2	ST 1/2
33	A625~A672	ST 1/2	ST 1/2	EST 1/2
34	A673~A720	EST 1/2	ST 1/2	ST 1/2
35	A721~A768	ST 1/2	EST 1/2	ST 1/2
36	A769~A816	EST 1/2	EST 1/2	EST 1/2
37	A817~A864	EST 1/2	ST 1/2	ST 1/2
38	A865~A888	ST 1	ST 1/2	ST 1/2
Best weight lb(kg)		**61844.7728(28052.3)**	**61183.313(27752.2)**	**60852.6106(27602)**

Table 4. Loading conditions for the 888-bar barrel vault

Node	Case 1			Case 2		
	Px kips(kN)	Py kips(kN)	Pz kips(kN)	Px kips(kN)	Py kips(kN)	Pz kips(kN)
2	0	0	−3.013(13.4)	0	−1.237(5.5)	−1.152(5.12)
14	0	0	−3.013(13.4)	0	−1.032(4.6)	−1.031(4.6)
28	0	0	−3.013(13.4)	0	−0.812(3.6)	-0.931(4.14)
62	0	0	−3.013(13.4)	0	−0.699(3.1)	−1.399(6.22)

6.3. Double arch barrel vault

The popularity of barrel vaults derived partly from the economy of these structures, as all arches can be constructed as identical members. At the same time, their cylindrical shape provided a great deal of volume under the roof, a distinct advantage for railway stations in the age of steam engines, or for large span warehouses, providing a welcome increase in their storage space.

For this bar barrel vault represented in Fig. 6, the material density is 0.288 lb/in^3 (7971.8 kg/m^3) and the modulus of elasticity is 30,450 ksi (210,000 MPa).

The members are subjected to the stress limits of +34.8, –22.5 ksi. Structural members of this barrel vault are kept and categorized into 44 groups. The minimum permitted cross-sectional area of each member is ST 1/2(0.25in^2) (1.61 cm^2) and the maximum cross-sectional area of each member is EST 4 (4.41 in^2) (28.45 cm^2). Table 6 provides the values and directions of the two load cases applied to the double arch barrel vault. The best weight of the CSS optimization is 20135.1966 lb (9133.1 kg), while it is 21903.2308 lb, (9935.1 kg), 20802.6448 lb (9435.9 kg), for the GA and PSO, respectively.

6.3.1. Configuration of the double arch barrel vault (Fig. 6(c)):

Inter radius = 503 in (1278 cm)
Outer radius = 562 in (1428 cm)
L=Length = 1063 in (2700 cm)
D=Span = 749.2 in (1903 cm)
H=Height = 167.3 in (425 cm)

The results of optimization are provided in Table 7. The convergence history of this barrel vault is shown in Fig. 7.

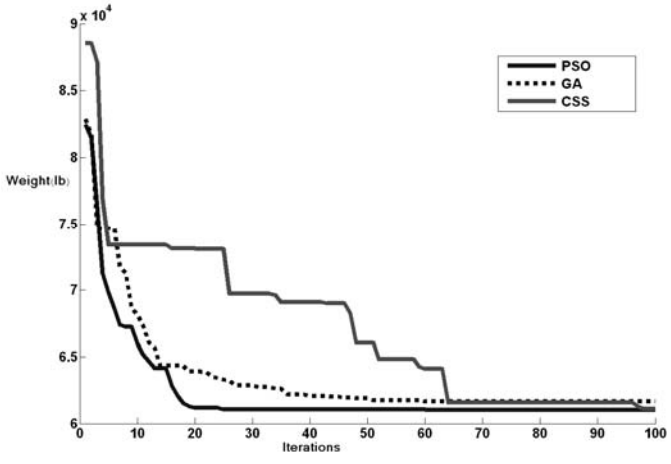

Fig. 5. The convergence history of the 888-bar barrel vault

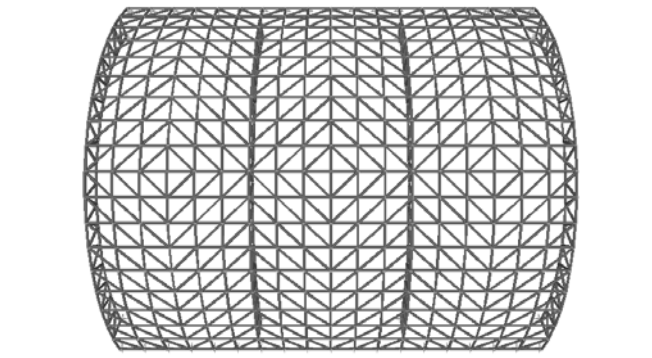

(a)

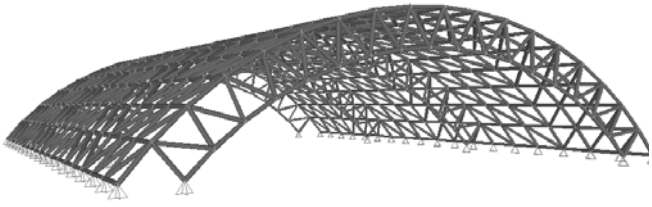

(b)

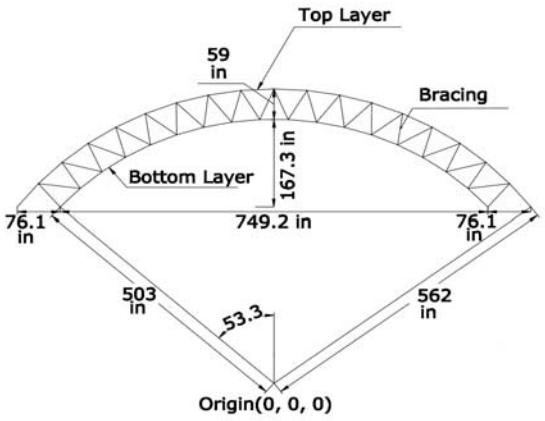

(c)

Fig. 6. (a) Top view of double arch barrel vault, (b) A front view of double arch barrel vault, (c) Configuration of double arch barrel vault

7. Concluding remarks

In this paper, the recently developed optimization approach CSS algorithm is applied to optimal design of barrel vaults. Several standard barrel vault examples from the literature are presented to demonstrate the effectiveness and robustness of the proposed approach compared with the other meta-heuristics. Compared to other meta-heuristics, CSS has less computing cost

Table 6. Loading conditions for the double arch barrel vault

Table 6. Loading conditions for the double arch barrel vault

Node	Case 1			Case 2		
	Px kips(kN)	Py kips(kN)	Pz kips(kN)	Px kips(kN)	Py kips(kN)	Pz kips(kN)
2	0	0	−0.5766(2.56)	0	0.132(0.59)	−0.6855(3.05)
9	0	0	−0.5766(2.56)	0	0.1192(0.53)	−0.700(3.11)

Table 7. Performance comparsion for the double arch barrel vault

	Element group	Optimal cross-sectional areas (in^2)		
		GA	PSO	CSS
1	A1~ A6	ST 1	ST 1 1/4	ST 3 1/2
2	A7~A12	EST 3 1/2	ST 4	EST 1 1/4
3	A13~A18	ST 1 1/4	EST 4	DEST 2
4	A19~A24	ST 1	EST 2	EST 1 1/4
5	A25~A30	EST 1/2	ST 1/2	ST 2 1/2
6	A31~A36	EST 3	ST 1 1/4	EST 4
7	A37~A42	EST 4	EST 1 1/4	ST 1 1/2
8	A43~A48	EST 1 1/4	ST 1/2	ST 1 1/4
9	A49~A60	EST 3	EST 2 1/2	ST 3/4
10	A61~A72	EST 1 1/4	ST 1/2	ST 2 1/2
11	A73~A84	DEST 2 1/2	ST 1	ST 1
12	A85~A96	DEST 2 1/2	ST 5	EST 2 1/2
13	A97~A108	ST 1/2	ST 2 1/2	ST 3/4
14	A109~A114	ST 3	DEST 2	EST 3/4
15	A115~A123	EST 2	EST 2 1/2	EST 1 1/4
16	A124~A132	ST 3 1/2	EST 2 1/2	EST 3 1/2
17	A133~A141	ST 1 1/4	EST 1 1/2	ST 2 1/2
18	A142~A150	DEST 2	ST 1 1/2	ST 1 1/4
19	A151~A159	EST 1/2	EST 3	ST 1
20	A160~A168	ST 1	ST 1 1 /4	EST 3/4
21	A169~A177	ST 3/4	ST 3/4	ST 1
22	A178~A186	ST 1	ST 1/2	EST 1 1/2
23	A187~A202	ST 1/2	ST 1/2	ST 1 /2
24	A203~A211	ST 3/4	ST 1/2	EST 1/2
25	A212~ A220	EST 1/2	ST 1/2	ST 1
26	A221~A229	EST 3/4	EST 4	DEST 3
27	A230~A238	EST 1/2	ST 1	ST 1/2
28	A239~A247	ST 1/2	ST 1/2	ST 1/2
29	A248~A256	ST 1/2	ST 1 1/4	ST 1
30	A257~A265	EST 1/2	ST 1/2	EST 1/2
31	A266~A274	ST 1	ST 1/2	EST 3/4
32	A275~A280	EST 3/4	ST 1/2	ST 1
33	A281~A290	ST 1/2	ST 1/2	ST 1/2
34	A291~A300	ST 1/2	ST 1/2	ST 1/2
35	A301~A310	ST 1/2	ST 1/2	EST 3/4
36	A311~A330	ST 1/2	ST 3/ 4	ST 3/4
37	A331~A350	ST 3/ 4	ST 3/4	ST 1 1/2
38	A351~A370	ST 3/4	ST 1/2	EST 1/2
39	A371~A390	ST 1/2	ST 1/2	EST 1/2
40	A391~A414	ST 1 /2	ST 1 /2	ST 1/2
41	A415~A424	ST 3	EST 3	ST 3/4
42	A425~A434	EST 2	EST 1 1/4	ST 1/2
43	A435~A444	ST 1 1/2	ST 1/2	ST 1 1/ 2
44	A445~A450	EST 3 1/2	EST 2 1/2	DEST 2
Best weight lb(kg)		**21903.2308(9935.1)**	**20802.6448(9435.9)**	**20135.1966(9133.1)**

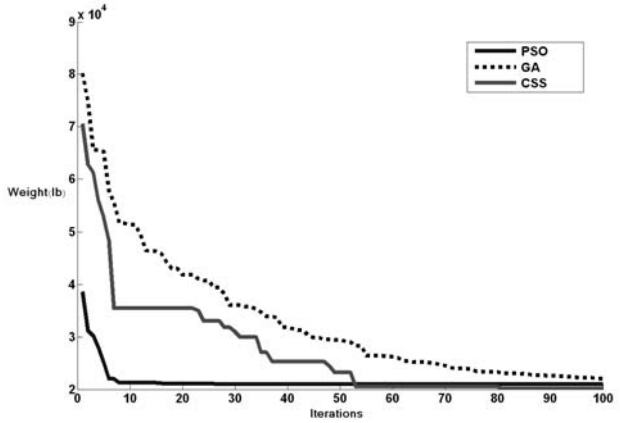

Fig. 7. The convergence history of the double arch barrel vault

and can determine the optimum results with a smaller number of analyses. Due to having a good balance between the exploration and exploitation, the performance of the CSS in both global search stage (initial iterations) and the local search stage (last iterations) is excellent. The comparison of the CSS results with those of the other heuristics shows the robustness of the present algorithm and demonstrates the efficiency of the algorithm to find optimum design of structures. The application of the present CSS algorithm is not limited to barrel vaults and can also be applied to other types of structural optimization problems, such as frame structures, and plates and shell type of structures.

Acknowledgement: The first author is grateful to Iran National Science Foundation for the support.

References

[1] Makowski, Z.S.: Analysis, Design, and Construction of Braced Barrel Vaults, Elsevier Applied Science Publishers, London, 1985.

[2] Fogel, L.J., Owens, A.J., Walsh, M.J.: Artificial Intelligence Through Simulated Evolution. John Wiley, Chichester, UK, 1966.

[3] Holland, J.H.: Adaptation in Natural and Artificial Systems. Ann Arbor, MI: University of Michigan Press, USA, 1975.

[4] Goldberg, D.E.: Genetic Algorithms in Search Optimization and Machine Learning. Addison-Wesley, Boston, MA, 1989.

[5] Glover, F.: Heuristic for integer programming using surrogate constraints. Decision Science 1977, Vol. 8, pp. 156–66.

[6] Dorigo, M., Maniezzo, V., Colorni, A.: The ant system: Optimization by a colony of cooperating agents. IEEE Trans Sys Man Cybernet B 1996 Vol. 26, pp. 29–41.

[7] Eberhart, R.C., Kennedy, J.: A new optimizer using particle swarm theory. Proceedings of the Sixth International Symposium on Micro Machine and Human Science, Nagoya, Japan, 1995.

[8] Kirkpatrick, S., Gelatt, C., Vecchi, M.: Optimization by simulated annealing. Science 1983, Vol. 220, pp. 671–680.

[9] Geem, Z.W.: Optimal design of water distribution networks using harmony search. PhD thesis, Korea University, South Korea, 2000.

[10] Erol, O.K., Eksin, I.: New optimization method: Big Bang–Big Crunch. Advances in Engineering Software 2006, Vol. 37, pp. 106–111.

[11] Kaveh, A., Talatahari, S.: A novel heuristic optimization method: charged system search, Acta Mechanica 2010, Vol. 213, pp. 267-286.

[12] Kaveh, A., Talatahari, S.: Optimal design of truss structures via the charged system search algorithm, Structural Multidisplinary Optimization 2010, Vol. 37, pp. 893-911.

[13] Kaveh, A., Talatahari, S.: Charged system search for optimum grillage systems design using the LRFD-AISC code, Journal of Constructional Steel Research, 2010, Vol. 66, pp. 767-771.

[14] Halliday, D., Resnick, R., Walker, J.: Fundamentals of Physics. 8th Edition, John Wiley and Sons, Inc., 2008.

[15] Kaveh, A., Sabzi, O.: A comparative study of two meta-heuristic algorithms for optimum design of reinforced concrete frames. International Journal of Civil Engineering, IUST, 2011, Vol. 9, pp. 193-206.

[16] Kaveh, A., Nasr, H.: Hybrid harmony search for conditional p-median problems, International Journal of Civil Engineering, IUST, 2012, Vol. 10, pp. 32-36..

[17] Kaveh, A., Shakouri Mahmud Abadi, A., Zolfaghari Moghaddam, S.: An adapted harmony search based algorithm for facility layout optimization, International Journal of Civil Engineering IUST, 2012, Vol. 10, pp. 37-42

[18] American Institute of Steel Construction (AISC): Manual of steel construction-allowable stress design. 9th ed. Chicago, IL, 1989.

[19] ASCE 7-05: Minimum Design Loads for Building and Other Structures, 2005.